Decoupled Voltage Stability Assessment of Distribution Networks Using Synchrophasors

Ali Bidadfar*, Hossein Hooshyar*, Mehdi Monadi‡, and Luigi Vanfretti*†
*KTH-Royal Institute of Technology, Stockholm, Sweden
†R&D Department, Statnett SF, Oslo, Norway
‡Technical University of Catalonia (UPC), Barcelona, Spain
Emails: bidadfar@kth.se, hossein.hooshyar@ee.kth.se, meh_monadi@yahoo.com, luigi.vanfretti@statnett.no

***Abstract*—This paper presents a real-time voltage stability assessment in distribution networks (DNs) capable of separating the effects of the transmission and distribution network by using synchronized phasor measurements. The method aims to assist transmission and distribution system operators to quantify the need of their services in different parts of the DN in order to provide adequate voltage support to their specific stakeholders. The method uses data from phasor measurement units (PMUs) to estimate models for both DN and transmission network (TN). A Thévenin equivalent model is estimated for the TN and a T-model for the DN. By applying the superposition theorem on these two models, the contribution of each network to the overall system voltage stability can be distinguished at a specific bus (equipped with a PMU). The method has been validated by a hardware-in-the-loop setup which consists an OPAL-RT real-time simulator and three PMUs.**

I. Introduction

Voltage stability assessment (VSA) helps in maintaining stable network operation and a secure voltage level through the entire power systems. The transition from passive to active DNs, brings challenges to available VSA methods because of underlying assumptions (passive loads) used to develop them. The necessity as well as the implementing procedure of VSA in developed DNs have been changed. As a matter of fact, many present DNs are loaded more heavily than ever before and they are undergoing fundamental changes in their constructions and operations; mainly because of the presence of distributed generation and power-electronic-based loads. Hence, a new real-time method to monitor and assess the voltage stability of DNs is necessary. Methods using network Thévenin equivalents (TEs) identified from synchrophasors have gained interest for their application to assess voltage stability in power systems [1], [2], [3]. Theoretically, to compute the TE seen from a given load bus, measurements of its voltage and currents are enough if the other loads, generation, and network topology are assumed to be constant. However, this assumption has been challenged in [4], which claims that using a single PMU, it is difficult to correctly identify a TE model because of variations at other load buses. This claim has been disproved in [2] by showing that it is possible to observe the effect of other load variations at single PMU locations. Moreover, [1] shows that obtaining a TE using two consecutive samples of a single PMU won't affect the precision of TE parameters because the sampling time interval with respect to time constraints of loads and generators is so small that the other loads and generators can be assumed to behave as time invariant components.

This paper presents a real-time VSA method applicable to DNs the utilize PMU data. The method is able to distinguish and separate the effects of the TN and DN on a voltage instability index (ISI) at a given load bus (equipped with a PMU). It is always important for transmission and distribution system operators (TSOs and DSOs) to know how their networks impact the voltage quality they supply to customers. In this sense, the proposed method assists the TSOs and DSOs to derive quantitative information of their networks' role in the system's voltage stability.

The method is founded on the load-line impedance-matching theory. Therefore, a TE circuit is identified at each load bus of interest, serving as a model of the entire power network. To separate the effects of transmission and distribution networks, the TE model identified for the entire power system is separated into two parts: a TN model (given by a new TE model) and a DN model (given by a T-circuit model). This separation allows to apply the superposition theorem on the ISI and to independently compute the effects of the TN and DN networks on this index.

The paper is organized as follows. The models for both networks are developed in II. Voltage stability analysis and separation of networks effects on ISI are explained respectively in II-C and III. The way of monitoring the analysis results is considered in IV, and real-time simulations and conclusions are made in V and VI.

II. Real-Time Equivalent Model and VSA

A. PMU Placement

One PMU is required for each load bus where VSA needs to be performed. This PMU is called secondary PMU and is labeled PMU2 in the figures below. Moreover, an additional PMU is required at the main substation of a DN, termed primary PMU and labeled PMU1. As shown in Fig. 1, PMU1 measures the voltage of the primary substation bus as well as the entire current flow of the DN of interest. PMU2 measures the voltage and current at the desired load bus. Additional secondary PMUs may exist for other load buses if their VSAs are interested; however, the primary PMU must always be at the primary substation. VSA at each desired load bus is

978-1-5090-4168-8/16/$31.00 ©2016 IEEE

performed using measurements from a secondary PMU and PMU1. The entire transmission network together with other DNs, i.e., other than the desired one, are lumped together and labled TN in Fig. 1.

B. Deriving Equations

By taking voltage and currents phasors from PMU2 a TE model seen from its corresponding load bus can be developed (see Fig. 2). Similarly, another TE representing the lumped TN model can be obtained from measurements of PMU1. To obtain a TE model seen from PMU2 a KVL equation is used: $\overline{E}_{th} = \overline{V}_L + \overline{Z}_{th}\overline{I}_L$, where $\overline{E}_{th}$ and $\overline{Z}_{th}$ are TE parameters, and $\overline{V}_L$ and $\overline{I}_L$ are voltage and current phasors at the desired load bus. Assuming that the TE parameters are constant between two consecutive data frames, $(\overline{V}_{L1}, \overline{I}_{L1})$ and $(\overline{V}_{L2}, \overline{I}_{L2})$, there will be two KVL equations with two unknowns $(\overline{E}_{th}, \overline{Z}_{th})$. The solution of these KVL equations results in (1) from where the TE parameters are computed. The subscript L in parameters stand for the desired load bus. Equations (1) can be used to formulate least-squares-error (LSQ) estimator where a window of data larger than two samples is used. However, the rate of change in the response of the network must be taken into account when the length of sampling window (number of samples) is determined. In the authors experience, in distribution systems where load variations are high, using 7 to 12 snapshots in the window yields satisfactory results (i.e., a rolling window of 120 240 ms of data).

$$\overline{Z}_{th} = \frac{\overline{V}_{L2} - \overline{V}_{L1}}{\overline{I}_{L1} - \overline{I}_{L2}} \ , \ \overline{E}_{th} = \frac{\overline{V}_{L2}\overline{I}_{L1} - \overline{V}_{L1}\overline{I}_{L2}}{\overline{I}_{L1} - \overline{I}_{L2}} \quad (1)$$

In addition to obtaining the TE parameters from measurements of PMU2, the impedance of the desired load is obtained as $\overline{Z}_L = \overline{V}_L/\overline{I}_L$. Moreover, a load model is needed to build power-voltage (PV) characteristics, as well as to decouple the TN and DN voltage stability effects. In this paper, an exponential model is used

$$P_L = P_{L0}\left(\frac{V_L}{V_{L0}}\right)^{\alpha} \ , \ Q_L = Q_{L0}\left(\frac{V_L}{V_{L0}}\right)^{\beta} \quad (2)$$

where P_L, Q_L, and V_L are fed from PMU2. The parameters P_{L0} and Q_{L0} are scheduled active and reactive power. V_{L0} is nominal voltage and α and β are exponential constants. P_{L0}, Q_{L0}, α and β are determined using LSQ method. The nominal voltage, V_{L0}, is assumed to be one per unit. The TE parameters of the TN, $\overline{E}_{tn}$ and $\overline{Z}_{tn}$, are derived from least-squares solution of equation (3), in which the samplings of the PMU1 are used.

$$\overline{Z}_{tn} = \frac{\overline{V}_{dn2} - \overline{V}_{dn1}}{\overline{I}_{dn1} - \overline{I}_{dn2}} \ , \ \overline{E}_{tn} = \frac{\overline{V}_{dn2}\overline{I}_{dn1} - \overline{V}_{dn1}\overline{I}_{dn2}}{\overline{I}_{dn1} - \overline{I}_{dn2}} \quad (3)$$

$\overline{V}_{dn}$ and $\overline{I}_{dn}$ are the voltage and current of the DN that are measured by PMU1.

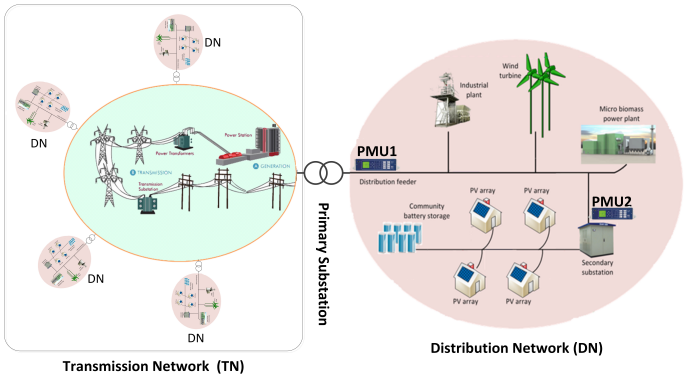

Fig. 1. Schematic diagram of PMUs placed in a distribution network

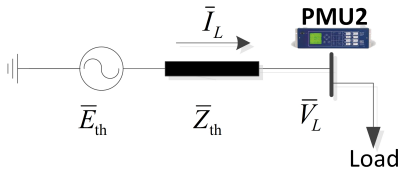

Fig. 2. Thévenin equivalent seen from a desired load

C. Voltage Stability Assessment

The voltage stability assessment (VSA) of a Thévenin equivalent circuit is based on the impedance matching criteria ($Z_L = Z_{th}$), where the voltage of the load reaches to its instability point. Using the impedance matching criterion, [5] derives a voltage stability index (SI) that is defined as $\text{SI} = 1 - Z_{th}/Z_L$. The index SI varies from one to zero when the system goes from a stable to an unstable condition. Using the SI, the complementary voltage instability index (ISI) is defined as inverse of SI, which varies from zero to one when the SI changes from one to zero. The ISI is given by

$$\text{ISI} = Z_{th}/Z_L. \quad (4)$$

As mentioned earlier, both TN and DN play roles in the voltage stability of each load inside the DN; however, for some loads the effect of one of either the TN or DN is zero. For instance, if there exist a local generator inside the DN supplying the entire demands, the TN does not influence the ISI of that bus (to a large degree). As another example, if a load is connected close to the primary substation and its current is supplied mostly by the TN, the DN will have little or no contribution on the ISI.

III. Separating the Effects of the TN and DN on ISI

The instability index of a desired load, ISI is divided into ISI_{tn} and ISI_{dn}, representing the effect of the TN and DN, respectively. These two components, expressed in (5), are calculated using the superposition theorem. To determine the ISI_{tn} the DN is disconnected from the primary substation point and the desired load is directly connected to this point

978-1-5090-4168-8/16/$31.00 ©2016 IEEE

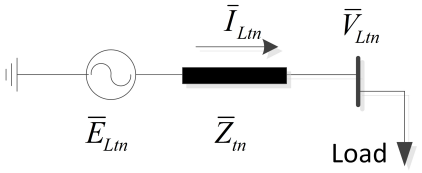

Fig. 3. The load is connected to TN to calculate the ISI_{tn}

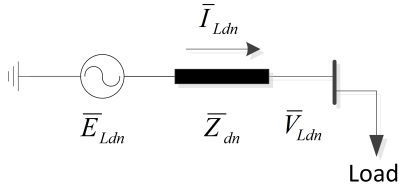

Fig. 4. The load is connected to DN to calculate the ISI_{dn}

as shown in Fig. 3. Next, by computing the ISI by (4), the ISI_{dn} can be calculated from (5).

$$\text{ISI} = ISI_{tn} + ISI_{dn} \tag{5}$$

A. Obtaining ISI_{tn}

As seen from Fig. 3 the DN has been disconnected, and thus its effect on the load instability is neglected. The corresponding index, ISI_{tn}, is given by

$$ISI_{tn} = Z_{tn}/Z_{Ltn}. \tag{6}$$

where Z_{Ltn} is the amplitude of load impedance when it is directly connected to the TN. It can be calculated from

$$Z_{Ltn} = V_{Ltn}^2/\sqrt{P_{Ltn}^2 + Q_{Ltn}^2} \tag{7}$$

where P_{Ltn} and Q_{Ltn} are the active and reactive power of the desired load when it is connected to the TN. These powers, and the voltage V_{Ltn}, are unknowns. They can be computed using the KVL equation of Fig. 3 and the load model (2). The voltage $\overline{E}_{Ltn}$ in Fig. 3 has the same amplitude as $\overline{E}_{tn}$ but it has a different phase angle. When the load is connected to TN its scheduled active and reactive powers, P_{L0} and Q_{L0}, are supposed to be the same as before; however, consumption powers, P_{Ltn} and Q_{Ltn}, differ as a consequence of voltage change (the load voltage has been changed from V_L to V_{Ltn}). The new amount of these powers are computed as

$$\begin{aligned} P_{Ltn} &= A_t\left[C_t cos(\delta_{Ltn}) - V_{Ltn}^2\right] + B_t C_t sin(\delta_{Ltn}) \\ Q_{Ltn} &= B_t\left[C_t cos(\delta_{Ltn}) - V_{Ltn}^2\right] - A_t C_t sin(\delta_{Ltn}) \end{aligned} \tag{8}$$

where $A_t = R_{tn}/Z_{tn}^2$, $B_t = X_{tn}/Z_{tn}^2$, and $C_t = V_{Ltn}E_{Ltn}$. The parameters R_{tn} and X_{tn} are the resistive and inductive part of the TN impedance. The load voltage, $\overline{V}_{Lth}$, is considered to have a zero phase angle; thus, the δ_{Ltn} in (8) is the phase angle of $\overline{E}_{Ltn}$. Combining (8) with the power-voltage relationship, results in (9), thereby canceling δ_{Ltn}.

$$\left(zp + \frac{R_{tn}}{Z_{tn}}V_{Ltn}^2\right)^2 + \left(zq + \frac{X_{tn}}{Z_{tn}}V_{Ltn}^2\right)^2 = E_{tn}^2 V_{Ltn}^2 \tag{9}$$

In (9), $zp = Z_{tn}P_{Ltn}$ and $zq = Z_{tn}Q_{Ltn}$. combining (9) and (2), results in three equations and three unknowns, V_{Ltn}, P_{Ltn}, and Q_{Ltn}. After solving these unknowns, the instability index ISI_{tn} can be determined from (6).

IV. Decoupled Voltage Stability Monitoring

The results from previous sections allow to estimate three PV curves: one for the TN, one for the DN, and one for the whole system. This provides intuitive way of understanding the effect of each network (TN and DN) on the voltage profile, and a graphical correlation with the three instability indexes. Observe that for the TN, equation (9) already provides the means to compute the PV curve for the TN.

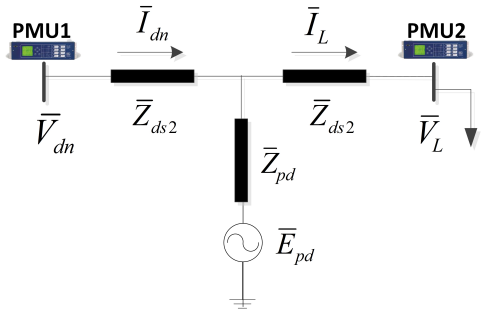

Fig. 5. T-model of DN used to derive $\overline{Z}_{dn}$

A. PV Characteristics for the Entire Network

The PV characteristics for the entire network depends on the current-voltage relationship of Fig. 2, which is similar to Fig. 3. Therefore, the characteristic will be obtained in similar same way as done for the entire network. Like (9), the PV characteristics of the entire network are

$$\left(tp + \frac{R_{th}}{Z_{th}}V_L^2\right)^2 + \left(tq + \frac{X_{th}}{Z_{th}}V_L^2\right)^2 = E_{th}^2 V_L^2 \tag{10}$$

where $tp = Z_{th}P_L$, $tq = Z_{th}Q_L$, and Q_L is replaced with (2). Plotting V_L in (10) against P_L results in the PV curve of the load considering the effects of both TN and DN networks.

B. PV Characteristic of the DN

To depict the PV curve of the desired load bus considering only the DN effect, i.e. where the effect of TN is omitted, a TE circuit which represents only the effect of DN is required, as shown in Fig. 4. The parameters of this circuit, $\overline{Z}_{dn}$ and $\overline{E}_{Ldn}$ are unknown. The $\overline{Z}_{dn}$ is determined from Fig. 5, where the DN has been modeled as a T-circuit using measurements from both PMUs. The T-model is estimated in two steps: first, the series impedances, $\overline{Z}_{ds1}$ and $\overline{Z}_{ds2}$, are determined; and second, shunt branch impedance is computed. The KVL equation of the series branches in Fig. 5, between two PMUs, is

$$-\overline{V}_{dn} + \overline{Z}_{ds1}\overline{I}_{dn} + \overline{Z}_{ds2}\overline{I}_L + \overline{V}_L = 0 \tag{11}$$

from where the series impedances can be computed using at least two measurements from each PMU. To calculate the

978-1-5090-4168-8/16/$31.00 ©2016 IEEE

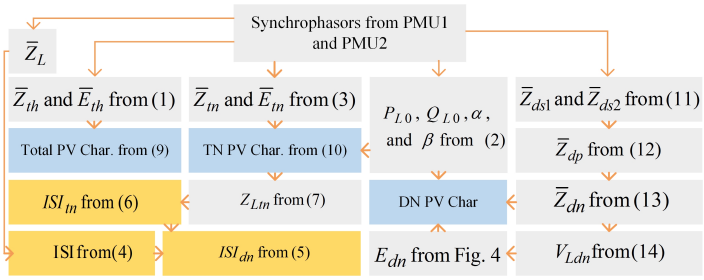

Fig. 6. The flowchart of the proposed method

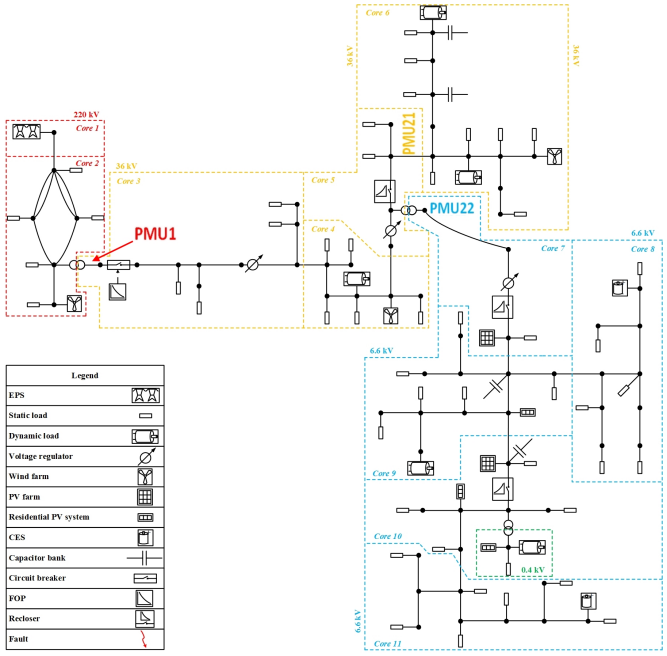

Fig. 7. IDE4L reference grid used for real-time simulations

shunt impedance $\overline{Z}_{pd}$, the equivalent model of power system seen from PMU2 in Fig. 5 must be the same as the one shown in Fig. 2. Therefore, by equating the total impedance seen from PMU2 with $\overline{Z}_{th}$, the $\overline{Z}_{pd}$ is given by

$$\overline{Z}_{th} = \left(\overline{Z}_{tn} + \overline{Z}_{ds1}\right) || \overline{Z}_{pd} + \overline{Z}_{ds2}. \quad (12)$$

Consequently, the Thévenin impedance of Fig. 4, $\overline{Z}_{dn}$ is obtained from $\overline{Z}_{ds1} || \overline{Z}_{pd} + \overline{Z}_{ds2} = \overline{Z}_{dn}$. The voltage $\overline{E}_{dn}$ in Fig. 4 cannot be obtained from Fig. 5, because by removing the TN effect the voltage at the interconnection of the DN, where PMU1 sits, will be unknown. Hence, to determine $\overline{E}_{dn}$, the load impedance Z_{Ldn} is calculated from the instability index, $Z_{Ldn} = Z_{dn}/ISI_{dn}$, where ISI_{dn} has already been obtained from (5). Next, the amplitude of load impedance has a relationship with the load voltage amplitude and apparent power amplitude S_{Ldn} as

$$Z_{Ldn} S_{Ldn} = V_{Ldn}^2. \quad (13)$$

The apparent power amplitude can be expressed as a function of the active and reactive power equivalent (2), resulting in

$$Z_{Ldn}\left(P_0^2\left(\frac{V_{Ldn}}{V_0}\right)^{2\alpha} + Q_0^2\left(\frac{V_{Ldn}}{V_0}\right)^{2\beta}\right)^{0.5} = V_{Ldn}^2 \quad (14)$$

where the only unknown, V_{Ldn}, can be computed. Note that the active and reactive power of the load are calculated from (2). By assuming a zero phase angle of voltage $\overline{V}_{Ldn}$, the load current in Fig. 4 is calculated as $\overline{I}_{Ldn} = \left(P_{Ldn} - jQ_{Ldn}\right)/V_{Ldn}$. By obtaining the current $\overline{I}_{Ldn}$, the voltage $\overline{E}_{dn}$ is obtained from Fig. 4 and finally the corresponding PV characteristics is determined in a similar way as for Fig. 2 and Fig. 3.

The whole process of calculating the indexes and PV characteristics is illustrated in the flowchart shown in Fig. 6.

V. Real-Time Testing

A. Power network model

The power system model used for the real-time simulation testing has been developed in the EU funded project, IDE4L [6]. As shown in Fig. 7, the model is a detailed active DN connected to a simplified TN. The entire system has three different voltage levels: high voltage (220 kV), medium voltage (36 kV), and low voltage (6.6 kV). As seen in the Fig. 7, PMU1 is placed at the main entrance of distribution network and two other PMUs measure voltages and currents of desired loads; PMU21 measures the entire 6.6 kV, and PMU22 measures the reminder of the network inside of Core 6.

B. Hardware-in-the-loop (HIL) testing setup

Fig. 8 illustrates the HIL setup used to test the VSA by PMU application using actual real-time synchrophasors. As shown, the measured voltages and currents are fed to PMUs through the analogue output ports of the OPAL-RT simulator. As indicated in the figure, three PMUs, which are SEL-421 from Schweitzer Engineering Laboratories, are used to compute phasors that are used as input for VSA function which is implemented on a LabVIEW platform using S^{3}DK [7].

C. Test Case A

In this case study, VSA of the low voltage network as well as the VSA of the network in Core 6, shown in Fig. 7, are performed. Because there are two PMUs within the DN, two individual T-models are derived. However, as noted before, there is always one TN model. In this simulation, the wind farm in Core 4 is disconnected, and the entire low voltage network is considered as an aggregated load seen from PMU22. Similarly, the network in Core 6 is an aggregated load as seen from PMU21. The PV curves and instability indexes are shown in Fig. 9 and Fig. 10. The figures show that the load measured by PMU21 is more stable than the loads measured by PMU22. The reason is that the low voltage network contains heavy loads which impose a voltage stress on core 6.

D. Test Case B

The simulation for test case A is repeated with the wind farm in Core 4 connected. Fig. 11 shows the results of this

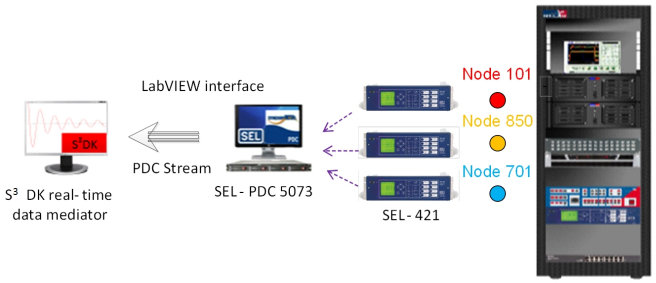

Fig. 8. Hardware-in-the-loop setup used for real-time simulations

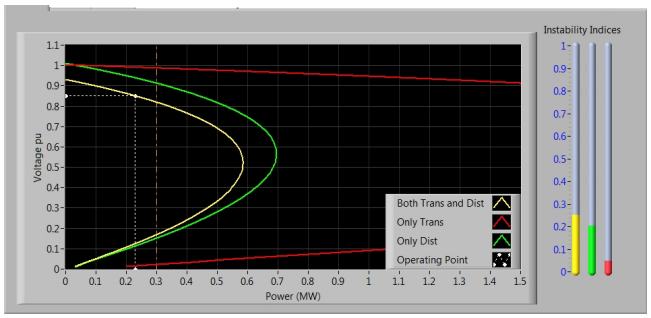

Fig. 9. VSA results of low voltage network seen from PMU22. The yellow bar shows ISI, the green one ISI_{dn}, and the red one ISI_{tn}

case study. Comparing Fig. 9 and Fig. 11, it is evident that the wind farm boosts the voltage stability margin, i.e., the three ISIs in Fig. 11 have been decreased and the maximum power of the load buses have been increased. Only through the proposed decoupling technique it is possible to discern that the voltage stability improvement is initiated from inside the distribution network. As seen from Fig. 11, the PV curve corresponding to distribution network has increased and with a smoother slope, which means that in a close nearby of the load the voltage is intensely supported.

The decoupled PV curves product of the simulations reveal the individual characteristics of both transmission and distribution networks, this is another advantage of the proposed decoupling method. The shape of the PV curve for the transmission network indicates, implicitly, that this network has a low series impedance, which results in robust voltage support. Unlike the transmission network, the distribution network has a high series impedance which causes a fairly steep slope the corresponding PV curves.

VI. Conclusion

A real-time voltage stability assessment method based on PMU measurements in distribution networks was introduced. The method is able to determine and separate the effects of distribution and transmission networks on the voltage stability of any desired load bus. To implement the method, one PMU, as know as PMU1, was used at the primary substation of a distribution network to derive a TE model to represent the transmission network. By using simultaneous measurements from PMU1 and each of the PMUs within a distribution

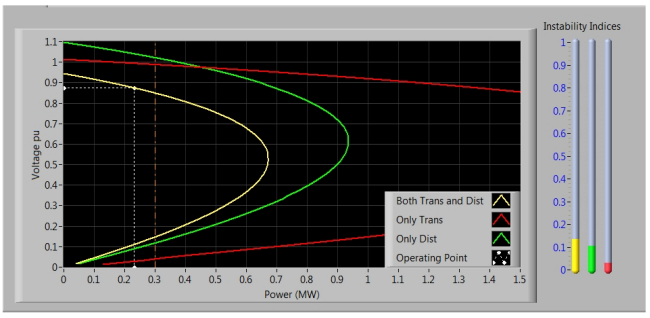

Fig. 10. VSA results of core 6 seen from PMU21. The yellow bar shows ISI, the green one ISI_{dn}, and the red one ISI_{tn}

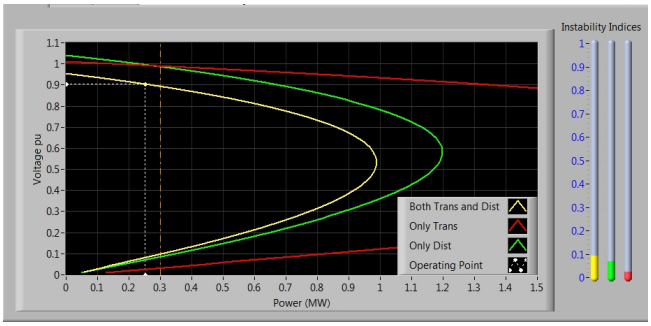

Fig. 11. VSA results of second case study. The yellow bar shows ISI, the green one ISI_{dn}, and the red one ISI_{tn}

network, a T-circuit equivalent is estimated between transmission network model and the load bus of interest. It was shown that by using these models, it is possible to split the voltage stability index into two parts, each reflecting the effects of different networks, and to visualize these effects on the PV curves. The method was implemented in a LabView application for real-time testing using actual PMU data. The functional performance of the application was tested by an HIL simulation setup.

References

[1] S. M. Abdelkader and D. J. Morrow, "Online tracking of thvenin equivalent parameters using pmu measurements," *IEEE Trans. Power Syst.*, vol. 27, no. 2, pp. 975–983, May 2012.

[2] J. H. Liu and C. C. Chu, "Wide-area measurement-based voltage stability indicators by modified coupled single-port models," *IEEE Trans. Power Syst.*, vol. 29, no. 2, pp. 756–764, March 2014.

[3] S. Corsi and G. N.Taranto, "A real-time voltage instability identification algorithm based on local phasor measurements," *IEEE Trans. Power Syst.*, vol. 23, no. 3, pp. 1271–1279, August 2008.

[4] Y. Wang, I. R. Pordanjani, W. Li, W. Xu, T. Chen, E. Vaahedi, and J. Gurney, "Voltage stability monitoring based on the concept of coupled single-port circuit," *IEEE Trans. Power Syst.*, vol. 26, no. 4, pp. 2154–2163, November 2011.

[5] G. A. Mahmood, "Voltage stability analysis of radial distribution networks using catastrophe theory," *IET Gener. Transm. Distrib.*, vol. 6, no. 7, pp. 612–618, 2012.

[6] H. Hooshyara, F. Mahmooda, L. Vanfretti, and M. Baudette, "Specification, implementation, and hardware-in-the-loop real-time simulation of an active distribution grid," *ELSEVIER, Sustainable, Energy, Grids, and Networks*, vol. 3, pp. 36–51, June 2015.

[7] L. Vanfretti, V. H. Arstrand, M. S. Almas, V. S. Peric, and J. O. Gjerde, "A software development toolkit for real-time synchrophasor application," in *IEEE PowerTech*, 2013.

978-1-5090-4168-8/16/$31.00 ©2016 IEEE